Cross sections for charge-changing processes involving kilo-electron-volt H and H^+ with CO and CO_2

B. G. Lindsay, W. S. Yu, and R. F. Stebbings
Department of Physics and Astronomy, and Rice Quantum Institute, Rice University, 6100 Main St., Houston, Texas 77005-1892, USA
(Received 21 October 2004; revised manuscript received 16 December 2004; published 8 March 2005)

Absolute differential cross sections are reported for electron capture and loss by 1–5 keV H atoms incident on CO and CO_2 for laboratory scattering angles up to 1.73°, and for charge transfer of 1–5 keV H^+ with CO and CO_2 for scattering angles up to 2.51°. To our knowledge, the H-atom differential electron-capture and -loss cross sections presented here are the first of their kind for CO and CO_2. The differential electron-loss cross sections are very similar to one another, and to previous measurements with other molecular targets, suggesting that some aspects of these collisions may be amenable to a relatively basic theoretical model. The differential measurements reported here significantly advance our knowledge of these collision processes and very good agreement is observed between the corresponding integral cross sections and prior work.

DOI: 10.1103/PhysRevA.71.032705 PACS number(s): 34.70.+e, 34.50.Lf

I. INTRODUCTION

Advances in our understanding of fundamental atomic collision phenomena depend heavily upon the availability of reliable experimental data; this is particularly true in areas where theory is relatively undeveloped. The various charge-changing processes involving keV H and H^+ in collision with atoms and molecules have been subject to quite extensive experimental investigation, but for CO and CO_2, there are significant gaps in our knowledge. Charge-changing cross sections for H and H^+ with CO and CO_2 have been measured by a number of prior investigators [1–21] and, in most cases, there is general agreement between the various studies as to the magnitude of the total cross sections. However, there are very few prior measurements for some of these processes and no prior H-CO_2 electron-capture data. Furthermore, to our knowledge, there are no published differential cross sections (DCSs) for electron capture or loss by H atoms for any of these targets; the only available DCS data are for charge transfer of H^+ at a single energy [18]. Here, absolute DCSs and corresponding integral cross sections are reported for electron capture and loss by 1–5 keV H-atoms incident on CO and CO_2 for laboratory scattering angles between 0.020° and 1.73°, and for charge transfer of 1–5 keV H^+ with CO and CO_2 for scattering angles between 0.026° and 2.51°.

It is worth noting that the reported data find direct application in models of the Martian atmosphere. Since Mars lacks an intrinsic magnetic field, its atmosphere, which is largely composed of CO_2 with smaller amounts of CO and other gases [22], is directly impacted by solar wind protons and by energetic H atoms formed via charge transfer [23]. Atmospheric models involving the interaction of the solar wind require knowledge of the processes studied here. The data presented are also pertinent to the interpretation of energetic neutral atom (ENA) measurements from the Mars Express spacecraft.

II. APPARATUS AND EXPERIMENTAL METHOD

The apparatus shown in Fig. 1 is used to measure H-atom electron-capture and -loss cross sections and H^+ charge-transfer cross sections, but the experimental procedures employed are significantly different and are described separately.

A. Electron-capture and -loss measurements

The experimental method has been described in detail previously [24,25]. H_2 is admitted to a magnetically confined plasma ion source. Ions are extracted from the source through a small aperture, accelerated, and focused to form a beam of the desired energy. Two confocal 60°-sector magnets are used to select H^+ ions which then enter a charge-transfer cell (CTC) where some of them are converted to fast neutral H atoms via charge transfer with krypton. At the energies studied here, the near-resonant H^+-Kr charge-transfer reaction produces predominantly ground-state hydrogen. A strong electric field (~400 V/cm) applied via deflection plates DP1 removes residual ions and also serves to quench any H(2*s*) metastables that may be present [24]. The neutral beam is collimated to an angular divergence of 0.006° by passage through a pair of laser-drilled apertures that form the exit of the CTC and the entrance to the target cell (TC). Following passage through the short target cell, the H beam impacts a position-sensitive detector (PSD1) located 68 cm beyond it. A set of deflection plates (DP2) is utilized to deflect fast product ions emerging from the target cell through an angle of approximately 5° onto a second position-sensitive detector (PSD2).

To measure the differential electron-capture or -loss cross section, CO or CO_2 is admitted to the target cell and the angles of scatter of the H^- or H^+ ions, formed through electron capture or loss by the primary H atoms, are determined from their positions of impact on PSD2. The H-atom flux incident on the target is determined by combining the number of H atoms that impact PSD1 with the number of ions produced. These measurements, together with the target number density, the target length, and the relative detection efficiency of the two PSDs are sufficient to determine the absolute differential and integral cross sections.

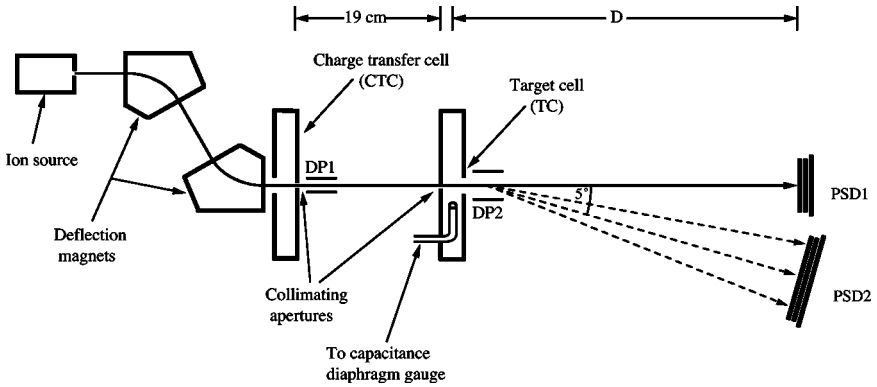

FIG. 1. Schematic of the apparatus. For the electron-capture and -loss cross section measurements D is 68 cm, and for the charge transfer measurements D is 32 cm. Note that the active detection area of PSD1 has a diameter of 25 mm and that of PSD2 has a diameter of 40 mm.

Measurement of the target number density and target length is straightforward but evaluation of the PSDs' relative detection efficiency requires careful consideration of the detectors' characteristics [26,27]. As discussed previously [25], it is accomplished by alternately deflecting an H^+ ion beam onto PSD1 and PSD2. In practice, the detection efficiencies are quite similar: PSD2's efficiency is 6-8% lower than that for PSD1, depending upon the energy of the incident ions.

Since the measured cross sections are generally small compared to those for reneutralization of the charged products, it is necessary to maintain conditions in the target cell so that the probability that a charged product ion is reneutralized is low. To this end, the pressure in the 1.46-mm-long target cell is maintained at 30 mtorr, which allows for reasonable count rates while keeping secondary collisions to an acceptable level. Corrections of approximately 10% are made to the electron-loss cross sections, utilizing the present charge transfer cross section data, to account for the loss of H^+ ions via this process. Corrections are not made to the electron-capture cross sections because information on electron loss by H^- ions is very limited [8,28] and, to our knowledge, there are no published cross sections at the relevant energies. The available data, however, do suggest that the magnitude of the correction needed for the electron-capture cross sections is also on the order of 10%.

Due to the finite angular range subtended by the detector it is not possible to collect all of the fast ionic products. The degree to which the integral cross section approximates the total cross section may, however, be estimated from the rapidity with which the DCS decreases with increasing scattering angle. This indicates that the present integral electron-capture cross sections, especially at the higher projectile energies, are a reasonable approximation to the total cross sections. By contrast, the slower decrease with angle of the electron-loss DCSs would seem to suggest that the corresponding integral cross sections should be viewed merely as lower limits to the total cross sections; this is discussed further in Sec. III.

B. Charge-transfer measurements

The experimental method has been described in detail previously [29]. A proton beam is generated as described in Sec. II A, however, for charge transfer, the CTC is evacuated and no electric field is applied between the DP1 deflection plates. The collimated proton beam therefore passes through the target cell and impacts PSD1. PSD1 serves to measure the flux of protons passing through the target cell and also to measure the scattered H-atom products. Note that, since PSD1 is physically smaller than PSD2, it is repositioned closer to the target cell so that data are collected over a comparable angular range to the electron-capture and -loss measurements.

In order to measure the differential charge-transfer cross section CO or CO_2 is admitted to the target cell and the angles of scatter of the neutral H atoms, formed by charge transfer of the primary H^+ ions, are determined from their positions of impact on PSD1. Unscattered primary H^+ ions are normally deflected away from PSD1 using deflection plates DP2 but are allowed to impact it periodically to assess the primary beam flux. These measurements, together with the target number density, obtained from the target gas pressure, and target length are sufficient to determine the absolute differential cross section. Note that the H^+ and H-atom detection efficiencies are identical within experimental uncertainties [30].

III. RESULTS: ELECTRON CAPTURE AND LOSS BY H ATOMS

The measured differential electron-capture and -loss cross sections are shown in Fig. 2 and selected values are tabulated in Tables I and II. Besides the statistical uncertainties shown on the graphs there are additional systematic uncertainties that range from ±10% to ±17% (Table III). The angular uncertainties arise from the finite primary beam size and the angular resolution used for analysis. From Fig. 2 it can be seen that, while all of the DCSs are forward peaked, electron-capture collisions tend to result in smaller scattering angles than electron-loss collisions. For the lowest energy studied, the DCSs decrease slowly with angle indicating that a significant fraction of the colliding particles is deflected through relatively large angles. There is no evidence of structure in the DCSs; the variations seen in the 1 keV electron-capture cross sections are almost certainly statistical in nature. At the moment, no other experimental data exist with which the present results may be directly compared.

One noteworthy feature of the CO and CO_2 electron-loss DCSs is their similarity to one another as illustrated in Fig. 3(a), and to DCSs for other molecular targets as shown in Fig. 3(b). It is also apparent that, above a few tenths of a

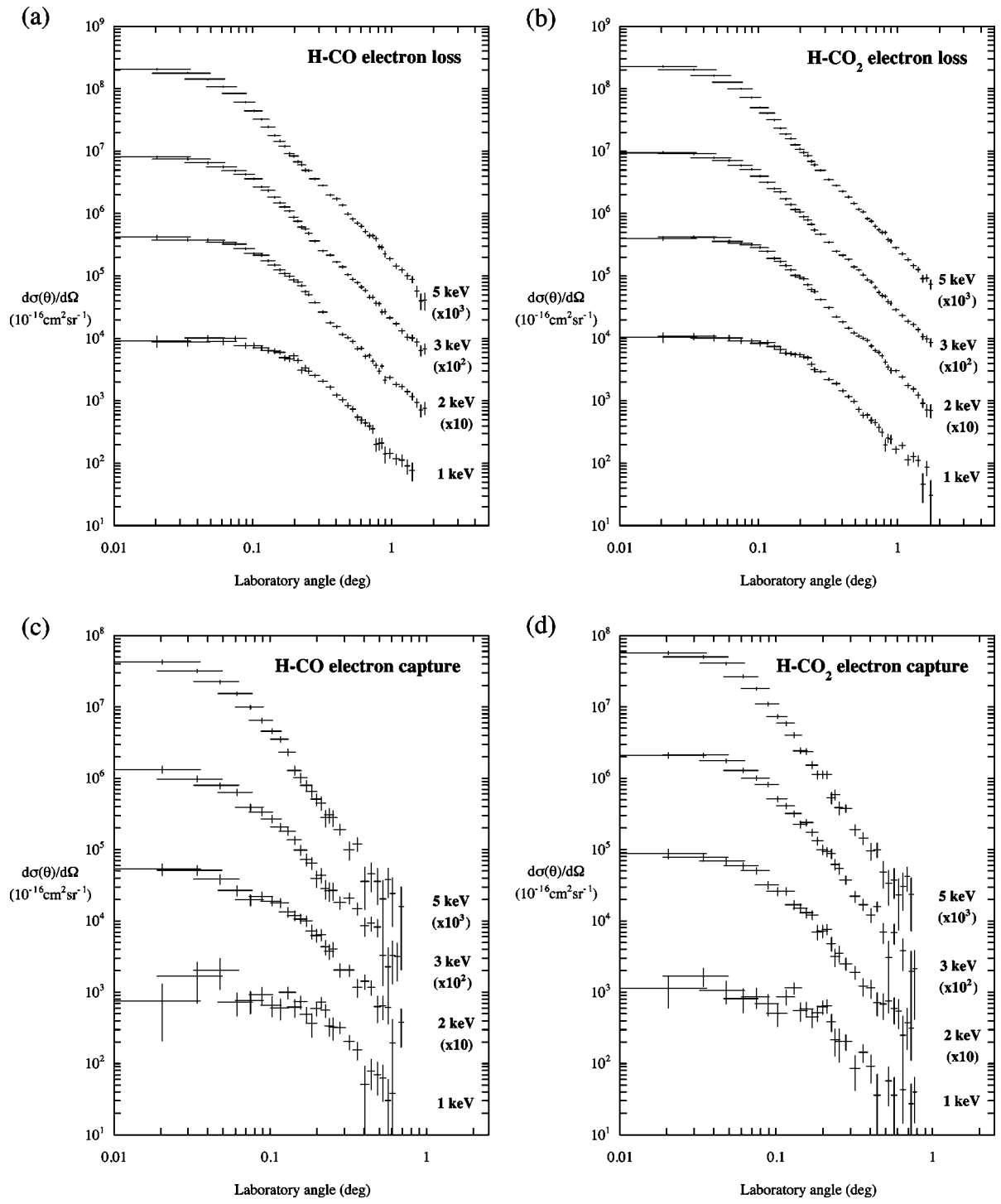

FIG. 2. Absolute differential cross sections for electron loss by H atoms in collisions with (a) CO, (b) CO_2; and for electron capture by H atoms in collisions with (c) CO, (d) CO_2. For convenience of presentation the data have been multiplied by the factors indicated.

degree, the DCSs fall on a common curve whose angular dependence parallels that of the $H-N_2$ direct scattering cross section [31]. This is in accord with the assertion by Van Zyl *et al.* [32] that the angular dependence of H-atom electron-loss and direct-scattering DCSs should be similar, except at small angles. Although theoretical approaches are not well enough developed to handle electron-capture and -loss collisions with any great degree of rigor [33], the strong resemblance between the various electron-loss DCSs suggests that it may be possible to describe some aspects of these collisions in terms of a single relatively basic scattering model.

The present integral cross sections and their associated uncertainties are tabulated in Table III. The uncertainties are primarily due to the PSD relative efficiency calibration, the uncertainty in the ratio of the H^+ to H-atom detection efficiencies, and to the repeatability of the measurements. The integral electron-loss data are compared to previous total measurements in Figs. 4(a) and 4(b). Note that the high-

TABLE I. Laboratory frame differential H-CO and H-CO_2 electron-loss cross sections, where E is the projectile energy and the numbers in square brackets represent powers of ten.

Laboratory angle θ (deg)	$d\sigma(\vartheta)/d\Omega$ (10^{-16} cm^2 sr^{-1})							
	H-CO				H-CO_2			
	E=1 keV	E=2 keV	E=3 keV	E=5 keV	E=1 keV	E=2 keV	E=3 keV	E=5 keV
0.020±0.015	9.12±1.83[3]	4.27±0.32[4]	8.10±0.40[4]	2.07±0.06[5]	1.06±0.19[4]	4.02±0.30[4]	9.57±0.42[4]	2.30±0.07[5]
0.048±0.015	1.02±0.12[4]	3.78±0.19[4]	6.57±0.24[4]	1.44±0.03[5]	1.03±0.12[4]	4.16±0.20[4]	7.95±0.26[4]	1.64±0.04[5]
0.075±0.015	1.00±0.09[4]	3.27±0.14[4]	4.93±0.16[4]	8.51±0.21[4]	9.19±0.87[3]	3.38±0.15[4]	5.99±0.18[4]	1.01±0.02[5]
0.116±0.015	7.11±0.65[3]	2.17±0.09[4]	2.71±0.10[4]	3.27±0.11[4]	8.68±0.67[3]	2.50±0.10[4]	3.21±0.11[4]	4.10±0.12[4]
0.157±0.015	6.06±0.53[3]	1.26±0.06[4]	1.51±0.06[4]	1.47±0.06[4]	5.87±0.49[3]	1.49±0.07[4]	1.73±0.07[4]	1.90±0.07[4]
0.198±0.015	5.27±0.44[3]	8.78±0.46[3]	8.85±0.43[3]	8.40±0.42[3]	5.58±0.43[3]	9.75±0.48[3]	1.07±0.05[4]	1.09±0.05[4]
0.252±0.015	3.03±0.30[3]	5.13±0.31[3]	4.85±0.28[3]	4.91±0.28[3]	3.15±0.29[3]	5.71±0.33[3]	5.50±0.30[3]	6.06±0.31[3]
0.320±0.025	2.09±0.13[3]	2.66±0.12[3]	2.55±0.11[3]	2.84±0.11[3]	2.23±0.13[3]	3.13±0.13[3]	3.51±0.12[3]	3.55±0.12[3]
0.402±0.025	1.23±0.10[3]	1.54±0.08[3]	1.68±0.08[3]	1.73±0.08[3]	1.46±0.10[3]	1.84±0.09[3]	2.17±0.09[3]	2.30±0.09[3]
0.484±0.025	8.57±0.78[2]	1.05±0.06[3]	1.07±0.06[3]	9.95±0.56[2]	9.93±0.74[2]	1.24±0.07[3]	1.41±0.07[3]	1.47±0.07[3]
0.607±0.025	4.97±0.62[2]	7.04±0.49[2]	6.75±0.44[2]	6.32±0.41[2]	5.97±0.58[2]	9.37±0.54[2]	8.79±0.48[2]	8.36±0.45[2]
0.893±0.025	1.42±0.41[2]	2.18±0.29[2]	2.71±0.26[2]	2.28±0.24[2]	2.47±0.41[2]	3.09±0.31[2]	3.73±0.29[2]	3.66±0.27[2]
1.405±0.056	7.73±2.48[1]	1.19±0.15[2]	1.03±0.12[2]	8.93±1.15[1]	1.13±0.23[2]	1.25±0.15[2]	1.40±0.13[2]	1.28±0.12[2]
1.732±0.056		7.73±1.74[1]	6.92±1.38[1]	4.14±1.28[1]	3.08±2.34[1]	7.12±1.71[1]	8.77±1.41[1]	7.50±1.32[1]

energy measurements of Toburen *et al.* [11] and Dimov and Dudnikov [8] are not shown. The overall agreement between the various measurements is quite good. The excellent agreement between the present 2 keV data and those of Smith *et al.* [16] and of McNeal [14] indicates that the present integral cross sections are very probably much closer to the total cross sections than might be expected from analysis of the DCSs (Sec. II A). The integral electron-capture data are shown in Figs. 4(c) and 4(d) together with those of Donahue and Husfar [4] and Pilipenko and Fogel [5]. The present data are in good accord with those of Pilipenko and Fogel [5]. While the large uncertainties associated with the Donahue and Hushfar [4] data make precise comparison difficult, their data are, nonetheless, not inconsistent with those presented here.

A few general comments on the data in Fig. 4 are in order. All of the cross sections are relatively small, certainly by comparison with typical near-resonant charge-transfer cross sections (Sec. IV), and they all decrease substantially with collision energy. Both of these phenomena derive from the fact that these H-atom electron-capture and -loss reactions are endothermic and require the input of roughly 14 eV in

TABLE II. Laboratory frame differential H-CO and H-CO_2 electron-capture cross sections, where E is the projectile energy and the numbers in square brackets represent powers of ten.

Laboratory angle θ (deg)	$d\sigma(\vartheta)/d\Omega$ (10^{-16} cm^2 sr^{-1})							
	H-CO				H-CO_2			
	E=1 keV	E=2 keV	E=3 keV	E=5 keV	E=1 keV	E=2 keV	E=3 keV	E=5 keV
0.020±0.015	7.66±5.58[2]	5.35±1.02[3]	1.34±0.16[4]	4.29±0.27[4]	1.14±0.54[3]	8.78±1.34[3]	2.11±0.20[4]	5.76±0.32[4]
0.048±0.015	2.04±0.48[3]	3.88±0.61[3]	7.98±0.82[3]	2.26±0.13[4]	1.06±0.37[3]	6.93±0.80[3]	1.77±0.12[4]	4.09±0.17[4]
0.075±0.015	7.68±2.67[2]	1.99±0.36[3]	3.93±0.45[3]	9.95±0.69[3]	8.65±2.72[2]	5.08±0.56[3]	1.01±0.07[4]	1.80±0.09[4]
0.116±0.015	6.07±1.97[2]	1.82±0.27[3]	2.10±0.27[3]	3.55±0.33[3]	8.73±2.10[2]	2.61±0.31[3]	4.11±0.38[3]	5.91±0.42[3]
0.157±0.015	7.39±1.57[2]	1.08±0.17[3]	9.93±1.60[2]	1.02±0.15[3]	5.88±1.41[2]	1.30±0.19[3]	2.42±0.25[3]	2.38±0.23[3]
0.198±0.015	5.97±1.27[2]	6.33±1.30[2]	3.97±1.04[2]	5.12±0.98[2]	6.28±1.34[2]	7.28±1.41[2]	1.01±0.15[3]	1.14±0.14[3]
0.252±0.015	3.26±1.13[2]	4.06±0.92[2]	2.68±0.72[2]	2.83±0.69[2]	2.06±1.00[2]	3.55±0.90[2]	5.48±0.97[2]	3.90±0.80[2]
0.320±0.025	2.05±0.48[2]	2.05±0.39[2]	2.11±0.37[2]	1.00±0.29[2]	8.67±4.47[1]	1.92±0.39[2]	2.23±0.39[2]	1.91±0.34[2]
0.402±0.025	5.14±4.11[1]	1.43±0.33[2]	8.63±2.49[1]	3.59±2.13[1]	9.30±3.95[1]	1.15±0.33[2]	1.23±0.28[2]	9.65±2.52[1]
0.484±0.025	7.07±3.45[1]	6.37±2.62[1]	8.27±2.26[1]	3.58±1.89[1]		6.92±2.74[1]	7.05±2.25[1]	4.90±1.98[1]
0.607±0.025	3.87±2.82[1]	1.96±1.96[1]	3.31±1.99[1]	2.43±1.60[1]		5.50±2.42[1]		2.34±1.60[1]

TABLE III. Absolute integral electron-capture and -loss cross sections for H atoms with CO and CO_2. The angular range for the integral cross sections is 0°–1.79°.

Energy (keV)	Electron loss (10^{-16} cm^2 sr^{-1})		Electron capture (10^{-17} cm^2 sr^{-1})	
	CO	CO_2	CO CO	CO_2
1	0.83±0.10	0.95±0.12	0.90±0.15	0.92±0.15
2	1.42±0.15	1.67±0.18	1.22±0.15	1.28±0.16
3	1.70±0.17	2.14±0.22	1.21±0.14	2.42±0.26
5	2.11±0.21	2.75±0.28	2.10±0.22	3.72±0.38

order to proceed. While the kinetic energy of the projectile is much greater than this, conversion of sufficient kinetic energy to internal energy requires close collisions and therefore results in comparatively small cross sections. Furthermore, as the collision energy decreases the energy needed for the reaction to take place represents a much larger fraction of the available kinetic energy and the cross section decreases considerably. Similar behavior is observed in highly nonresonant charge-transfer collisions [34]. These energy arguments alone do not explain why the electron-capture cross sections are so much smaller than those for electron loss. It seems reasonable to suppose that the electron-capture cross sections are smaller than the electron-loss cross sections because of the additional requirement that an H^- ion be formed.

IV. RESULTS: CHARGE TRANSFER OF H^+ IONS

The measured differential charge transfer cross sections are shown in Fig. 5 and selected values are tabulated in Table IV. Besides the statistical uncertainties shown on the graphs there are additional systematic uncertainties that range from ±6% to ±9% (Table V). All of the DCSs are strongly forward peaked as might be expected given the small energy defects for these reactions [18]. Both DCSs exhibit oscillatory structure at the lowest energies. This structure has been attributed to a combination of various interference effects by Gao *et al.* [18] whose 1.5 keV DCS data are shown for comparison. No structure is seen in the higher energy DCSs, perhaps because of the multiplicity of available scattering channels at these energies.

Also shown in Fig. 5(a) is the 1.5-keV DCS calculated by Kimura *et al.* [35] using the molecular orbital (MO) approach. While the general trend of the calculated cross section is consistent with the experimental data, there are important differences: the experimental cross section has a peak at 0.09 degrees but the theoretical curve dips at this angle; also, the sharp dip in the calculated curve at 0.2° is entirely absent from the experimental data. It seems improbable that

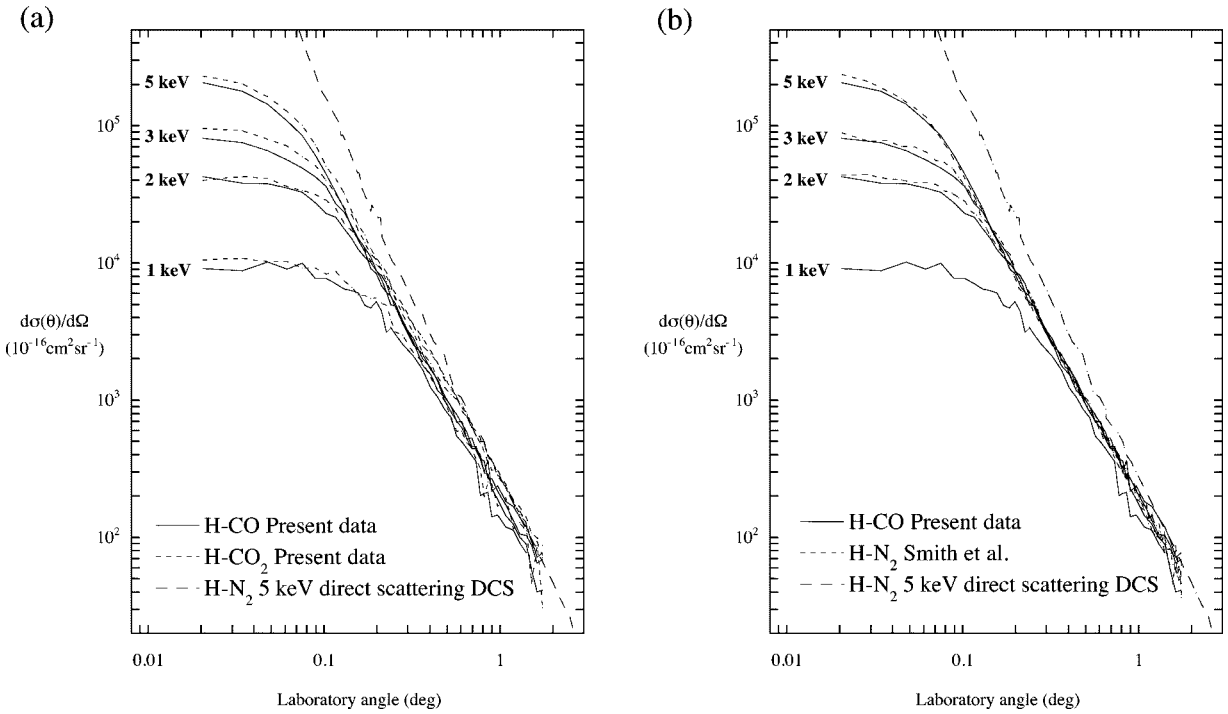

FIG. 3. Comparison of the present H-CO electron-loss DCSs with (a) those for H-CO_2, and (b) those for H-N_2 reported by Smith *et al.* [24]. The H-N_2 direct scattering cross section is also shown [31].

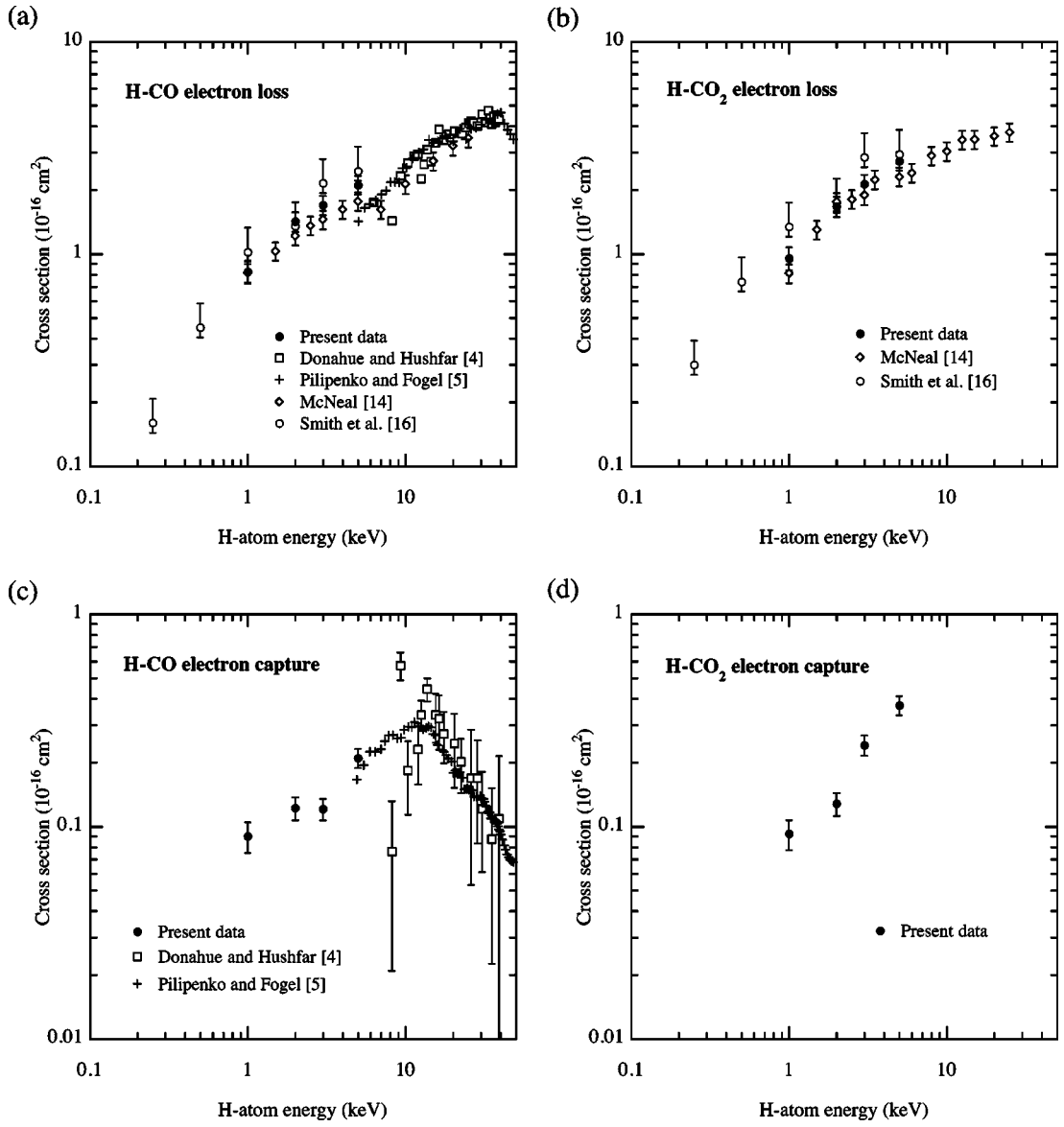

FIG. 4. Integral cross sections for electron loss by H atoms in collisions with (a) CO, (b) CO_2; and for electron capture by H atoms in collisions with (c) CO, (d) CO_2. Previous total cross section measurements are shown for comparison.

these discrepancies are entirely attributable to the finite angular resolution of the measurements. Furthermore, the regular oscillations seen in the theoretical curve for angles greater than 0.4 degrees are not observed in the experimental data.

TABLE V. Absolute integral cross sections for charge transfer of H^+ with CO and CO_2. The angular range for the integral cross sections is 0°–2.58°.

Energy (keV)	Charge transfer (10^{-16} cm^2 sr^{-1})	
	CO	CO_2
1	16.51±1.49	14.96±1.35
2	15.81±0.95	13.56±0.81
3	14.93±0.90	13.31±0.80
5	14.27±0.86	12.87±0.77

In this case, the angular resolution of the measurements would, to a significant extent, mask such oscillations. However, it is possible that the oscillations may simply result from the limitations inherent in the calculations themselves [35]; in a recent study, Cabrera-Trujillo *et al.* [36] demonstrated that similar oscillations were due to just such a cause.

The fact that the DCSs are so strongly forward peaked means that virtually all of the scattered H-atom products are detected and therefore the present integral cross sections are essentially equal to total cross sections, and they are therefore compared to the previous total measurements in Fig. 6. Note that high-energy measurements [7,10,11] and those subject to very large uncertainties [15], are not shown on this figure. Likewise, the data of Shah and Gilbody [19], which are normalized to those of Rudd *et al.* [17] and cover a similar energy range, and those of Browning and Gilbody [9], which include additional contributions due to ionization, are not shown. Apart from the scatter in the 5 keV H-CO_2

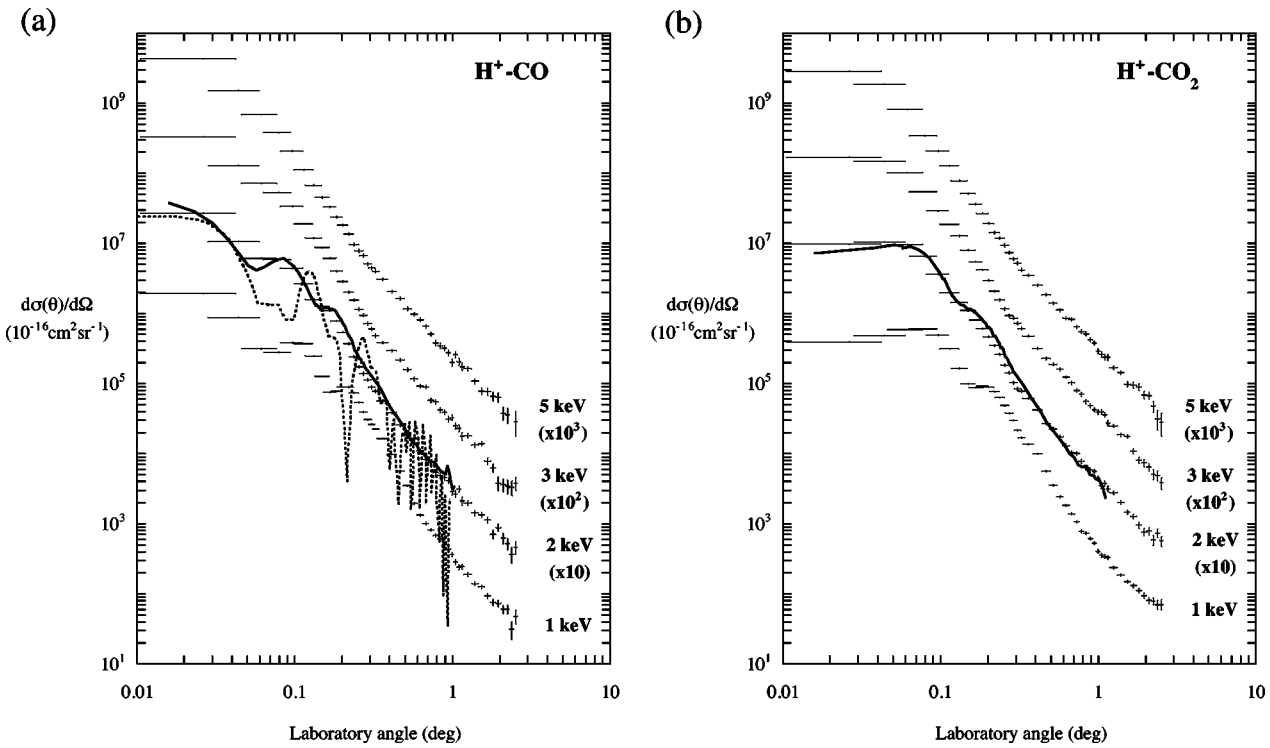

FIG. 5. Absolute differential cross sections for charge transfer of H^+ with (a) CO and (b) CO_2. The 1.5 keV DCS data of Gao *et al.* [18], shown as a solid line, and the 1.5-keV calculations of Kimura *et al.* [35], shown as a dashed line, are plotted for comparison with the present 2 keV data. For convenience of presentation the data have been multiplied by the factors indicated.

TABLE IV. Laboratory frame differential H^+-CO and H^+-CO_2 charge transfer cross sections, where E is the projectile energy and the numbers in square brackets represent powers of ten.

	$d\sigma(\vartheta)/d\Omega$ (10^{-16} cm^2 sr^{-1})							
Laboratory angle θ (deg)	H^+-CO				H^+-CO_2			
	E=1 keV	E=2 keV	E=3 keV	E=5 keV	E=1 keV	E=2 keV	E=3 keV	E=5 keV
0.026±0.016	1.93±0.02[6]	2.72±0.03[6]	3.33±0.03[6]	4.27±0.03[6]	3.93±0.08[5]	9.76±0.17[5]	1.70±0.02[6]	2.88±0.02[6]
0.044±0.016	8.84±0.09[5]	1.07±0.01[6]	1.29±0.01[6]	1.53±0.01[6]	4.88±0.07[5]	1.06±0.01[6]	1.49±0.01[6]	1.88±0.02[6]
0.061±0.016	3.17±0.05[5]	6.17±0.09[5]	7.21±0.09[5]	6.93±0.08[5]	5.90±0.06[5]	9.64±0.11[5]	1.02±0.01[6]	8.22±0.08[5]
0.079±0.016	2.84±0.04[5]	5.91±0.08[5]	5.35±0.07[5]	3.85±0.05[5]	6.10±0.06[5]	6.60±0.08[5]	5.45±0.07[5]	3.44±0.05[5]
0.096±0.016	3.88±0.04[5]	4.44±0.06[5]	3.38±0.05[5]	2.08±0.04[5]	4.94±0.05[5]	3.66±0.05[5]	2.91±0.04[5]	2.10±0.03[5]
0.114±0.016	3.75±0.04[5]	2.67±0.05[5]	1.91±0.03[5]	1.13±0.02[5]	3.14±0.03[5]	2.00±0.04[5]	1.88±0.03[5]	1.29±0.02[5]
0.149±0.016	1.28±0.02[5]	1.27±0.03[5]	8.79±0.20[4]	4.56±0.13[4]	9.97±0.16[4]	1.11±0.02[5]	8.06±0.18[4]	5.19±0.14[4]
0.202±0.016	9.02±0.14[4]	5.42±0.15[4]	2.87±0.10[4]	1.84±0.07[4]	8.86±0.13[4]	4.69±0.13[4]	2.99±0.10[4]	1.94±0.07[4]
0.254±0.016	5.39±0.09[4]	1.74±0.08[4]	1.16±0.06[4]	7.89±0.44[3]	4.89±0.09[4]	1.86±0.08[4]	1.18±0.05[4]	9.44±0.46[3]
0.324±0.016	2.27±0.05[4]	7.86±0.46[3]	4.86±0.32[3]	4.05±0.28[3]	1.70±0.05[4]	7.87±0.44[3]	6.13±0.34[3]	4.19±0.27[3]
0.412±0.029	9.78±0.18[3]	3.90±0.17[3]	2.98±0.13[3]	2.06±0.10[3]	1.00±0.02[4]	4.25±0.17[3]	3.19±0.13[3]	2.56±0.11[3]
0.570±0.029	1.97±0.07[3]	1.65±0.10[3]	1.17±0.07[3]	9.83±0.62[2]	2.44±0.08[3]	1.76±0.09[3]	1.62±0.08[3]	1.13±0.06[3]
0.885±0.029	5.07±0.31[2]	4.60±0.45[2]	3.93±0.34[2]	3.24±0.31[2]	6.23±0.33[2]	5.94±0.47[2]	4.88±0.36[2]	4.23±0.32[2]
1.385±0.071	1.41±0.09[2]	1.44±0.13[2]	1.34±0.11[2]	1.09±0.10[2]	1.87±0.10[2]	2.03±0.14[2]	1.88±0.12[2]	1.45±0.10[2]
1.806±0.071	7.67±0.82[1]	7.11±0.98[1]	6.30±0.86[1]	6.64±0.97[1]	1.13±0.09[2]	9.64±0.97[1]	8.15±0.87[1]	8.97±0.97[1]
2.507±0.071	4.83±1.05[1]	4.66±1.01[1]	3.83±0.80[1]	2.89±1.12[1]	7.13±1.13[1]	5.76±0.96[1]	3.89±0.76[1]	2.82±1.02[1]

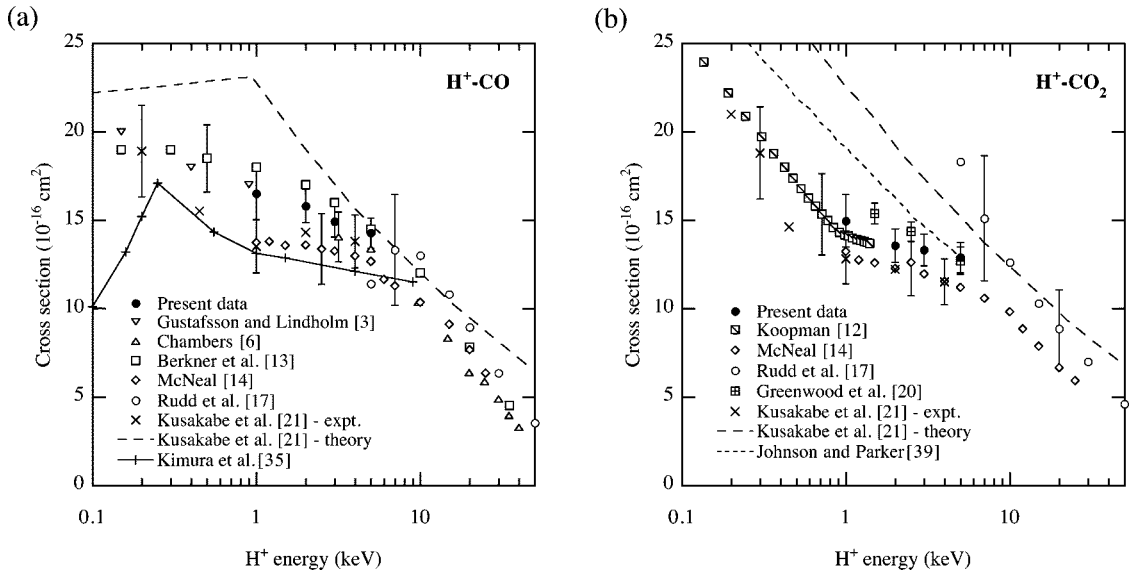

FIG. 6. Integral cross sections for charge transfer of H^+ with (a) CO, and (b) CO_2 together with previous total cross section measurements. Berkner, Pyle, and Stearns [13] actually measured cross sections for D^+ and their data are therefore plotted at the equivalent proton energy.

data, which is clearly due to the large uncertainty associated with the Rudd *et al.* [17] measurement at this particular energy, there is good agreement between the various studies for both targets. The integral cross sections reported by Gao *et al.* [18] are also consistent with the measurements in Fig. 6 [37].

The large magnitudes and the energy dependences of these total cross sections (Fig. 6) are consistent with the near-resonant nature of the reactions. Furthermore, the fact that the CO_2 cross section continues to increase rapidly at the lowest energies, in contrast with the behavior of the CO cross section, is a consequence of the significantly smaller energy defect for the CO_2 reaction. It is to be noted that, with the present apparatus, it is not possible to distinguish between simple charge-transfer and transfer ionization; although it seems very unlikely that transfer ionization will be significant at these relatively low collision energies. Also, while some fraction of the slow product ions undoubtedly dissociate, our apparatus provides no information on their fate. According to Browning and Gilbody [9], the majority of the CO^+ product ions do not dissociate at the energies studied here and the fraction that do increases with increasing energy.

In addition to the various experimental investigations, the H^+-CO calculations of Kimura *et al.* [35] and those performed by Kusakabe *et al.* [21] using the Olson formula [38] are shown in Fig. 6(a). The Kimura *et al.* [35] cross section reproduces the measured cross section quite well, and better than that resulting from the use of the Olson formula, which tends to overestimate it. It is worth noting that the discrepancies between the calculated and measured total cross sections are relatively small when compared to the discrepancies seen between the corresponding DCSs in Fig. 5. In the latter case, the discrepancies exceed an order of magnitude at certain angles, thus clearly demonstrating that the DCS can provide a more sensitive test of the theory than the total cross section.

The H^+-CO_2 calculations of Kusakabe *et al.* [21] and those of Johnson and Parker [39], also based on the work of Olsen *et al.* [38,40], are shown in Fig. 6(b). Perhaps not surprisingly they both exhibit a similar monotonic energy dependence, and neither reproduces the plateau that is observed in the 1–5 keV region. Kusakabe *et al.* [21] have advanced some suggestions as to the origin of the structure in this particular energy dependence curve, however, without more information these must remain speculations.

V. CONCLUSION

Absolute differential cross sections are reported for electron capture and loss by 1–5 keV H atoms incident on CO and CO_2 for laboratory scattering angles up to 1.73°, and for charge transfer of 1–5 keV H^+ with CO and CO_2 for scattering angles up to 2.51°. To our knowledge, the H-atom differential electron capture and loss cross sections presented here are the first of their kind for CO and CO_2. The differential electron-loss cross sections are very similar to one another, and to previous measurements with other molecular targets, suggesting the possibility that some aspects of these collisions may be amenable to a relatively basic theoretical model. The differential measurements reported here significantly advance our knowledge of these collision processes and very good agreement is observed between the corresponding integral cross sections and prior work.

ACKNOWLEDGMENTS

We gratefully acknowledge support by the National Science Foundation under Grant No. 0108734 and by the Robert A. Welch Foundation. We would also like to acknowledge useful communications with Pontus Brandt.

[1] Y. Nakai, T. Shirai, T. Tabata, and R. Ito, At. Data Nucl. Data Tables **37**, 69 (1987).
[2] H. B. Gilbody and J. B. Hasted, Proc. R. Soc. London, Ser. A **238**, 334 (1956).
[3] E. Gustafsson and E. Lindholm, Ark. Fys. **18**, 219 (1960).
[4] T. M. Donahue and F. Hushfar, Phys. Rev. **124**, 138 (1961).
[5] D. V. Pilipenko and Ya. M. Fogel, Sov. Phys. JETP **15**, 646 (1962).
[6] E. S. Chambers, Report No. UCRL-14214 University of California, 1965.
[7] J. Desesquelles, G. D. Cao, and M. Dufay, C. R. Seances Acad. Sci., Ser. B **262**, 1329 (1966).
[8] G. I. Dimov and V. G. Dudnikov, Sov. Phys. Tech. Phys. **11**, 919 (1967).
[9] R. Browning and H. B. Gilbody, J. Phys. B **1**, 1149 (1968).
[10] M. C. Poulizac, J. Desesquelles, and M. Dufay, Ann. Astrophys. **30**, 301 (1967).
[11] L. H. Toburen, M. Y. Nakai, and R. A. Langley, Phys. Rev. **171**, 114 (1968).
[12] D. W. Koopman, Phys. Rev. **166**, 57 (1968).
[13] K. H. Berkner, R. V. Pyle, and J. W. Stearns, Nucl. Fusion **10**, 145 (1970).
[14] R. J. McNeal, J. Chem. Phys. **53**, 4308 (1970).
[15] M. A. Coplan and K. W. Ogilvie, J. Chem. Phys. **52**, 4154 (1970).
[16] K. A. Smith, M. D. Duncan, M. W. Geis, and R. D. Rundel, J. Geophys. Res. **81**, 2231 (1976).
[17] M. E. Rudd, R. D. DuBois, L. H. Toburen, C. A. Ratcliffe, and T. V. Goffe, Phys. Rev. A **28**, 3244 (1983).
[18] R. S. Gao, L. K. Johnson, C. L. Hakes, K. A. Smith, and R. F. Stebbings, Phys. Rev. A **41**, 5929 (1990).
[19] M. B. Shah and H. B. Gilbody, J. Phys. B **23**, 1491 (1990).
[20] J. B. Greenwood, A. Chutjian, and S. J. Smith, Astrophys. J. **529**, 605 (2000).
[21] T. Kusakabe, K. Asahina, J. P. Gu, G. Hirsch, R. J. Buenker, M. Kimura, H. Tawara, and Y. Nakai, Phys. Rev. A **62**, 062714 (2000).
[22] R. Rodrigo, E. García-Álvarez, M. J. López-González, and J. J. López-Moreno, J. Geophys. Res., [Solid Earth Planets] **95**, 14795 (1990); H. Nair, M. Allen, A. D. Anbar, and Y. L. Yung, Icarus **111**, 124 (1994).
[23] E. Kallio and S. Barabash, J. Geophys. Res., [Space Phys.] **106**, 165 (2001).
[24] G. J. Smith, L. K. Johnson, R. S. Gao, K. A. Smith, and R. F. Stebbings, Phys. Rev. A **44**, 5647 (1991).
[25] B. G. Lindsay, W. S. Yu, K. F. McDonald, and R. F. Stebbings, Phys. Rev. A **70**, 042701 (2004).
[26] R. S. Gao, P. S. Gibner, J. H. Newman, K. A. Smith, and R. F. Stebbings, Rev. Sci. Instrum. **55**, 1756 (1984).
[27] H. C. Straub, M. A. Mangan, B. G. Lindsay, K. A. Smith, and R. F. Stebbings, Rev. Sci. Instrum. **70**, 4238 (1999).
[28] D. V. Pilipenko, V. A. Gusev and Ya. M. Fogel, Sov. Phys. JETP **22**, 965 (1966); I. Kovacs, Nucl. Instrum. Methods **51**, 224 (1967).
[29] B. G. Lindsay, D. R. Sieglaff, D. A. Schafer, C. L. Hakes, K. A. Smith, and R. F. Stebbings, Phys. Rev. A **53**, 212 (1996).
[30] R. S. Gao, L. K. Johnson, D. A. Schafer, J. H. Newman, K. A. Smith, and R. F. Stebbings, Phys. Rev. A **38**, 2789 (1988); L. K. Johnson, R. S. Gao, C. L. Hakes, K. A. Smith, and R. F. Stebbings, *ibid.* **40**, 4920 (1989).
[31] J. H. Newman, Y. S. Chen, K. A. Smith, and R. F. Stebbings, J. Geophys. Res., [Space Phys.] **91**, 8947 (1986); L. K. Johnson, R. S. Gao, K. A. Smith, and R. F. Stebbings, Phys. Rev. A **38**, 2794 (1988).
[32] B. Van Zyl, T. Q. Le, H. Neumann, and R. C. Amme, Phys. Rev. A **15**, 1871 (1977); H. Neumann, T. Q. Le, and B. Van Zyl, *ibid.* **15**, 1887 (1977).
[33] H. Levy II, Phys. Rev. **185**, 7 (1969); D. R. Bates and A. Williams, Proc. Phys. Soc., London, Sect. A **70**, 306 (1957).
[34] B. G. Lindsay and R. F. Stebbings, Phys. Rev. A **67**, 022715 (2003).
[35] M. Kimura, J.-P. Gu, G. Hirsch, R. J. Buenker, and P. C. Stancil, Phys. Rev. A **61**, 032708 (2000).
[36] R. Cabrera-Trujillo, Y. Öhrn, E. Deumens, J. R. Sabin, and B. G. Lindsay, Phys. Rev. A **70**, 042705 (2004).
[37] Note that the CO and CO_2 integral cross sections are stated incorrectly in Table I of the Gao *et al.*, (Ref. [18]) paper: $\sigma(H^+\text{-}CO)$ should be 14 $Å^2$, and $\sigma(H^+\text{-}CO_2)$ should be 12 $Å^2$.
[38] R. E. Olson, Phys. Rev. A **6**, 1822 (1972).
[39] C. A. F. Johnson and J. E. Parker, Chem. Phys. **111**, 307 (1987).
[40] R. E. Olson, F. T. Smith, and E. Bauer, Appl. Opt. **10**, 1848 (1971); R. E. Olson and F. T. Smith, Phys. Rev. A **7**, 1529 (1973); G. E. Ice and R. E. Olson, *ibid.* **11**, 111 (1975).